mone may be involved in receptor binding for both classes of receptors. By analogy with GH and GM-CSF, this would indicate that the exposed surface of helix D or the residues on the "side" of the bundle on helices A and C are most likely to be implicated in receptor binding.

It seems that a four-helical bundle with the distinctive "double-overhand" topology is a common structural scaffolding adopted by all the cytokines that bind receptors belonging to the hematopoietic superfamily and subclass III receptor tyrosine kinases. This structural motif is preserved across a diverse array of hormones that often possess no detectable sequence homology.

REFERENCES AND NOTES

1. N. A. Nicola, *Annu. Rev. Biochem.* **58**, 45 (1989); S. C. Clark and R. Kamen, *Science* **236**, 1229 (1987).
2. E. R. Stanley, L. J. Guilbert, R. J. Tushinsky, S. H. Bartelmez, *J. Cell. Biochem.* **21**, 151 (1983).
3. P. Ralph *et al.*, *Immunobiology* **172**, 194 (1986).
4. C. J. Sherr *et al.*, *Cell* **41**, 665 (1985).
5. E. S. Kawasaki *et al.*, *Science* **230**, 291 (1985).
6. G. G. Wong *et al.*, *ibid.* **235**, 1504 (1987).
7. D. P. Cerretti *et al.*, *Mol. Immunol.* **25**, 761 (1988).
8. E. S. Kawasaki and M. B. Ladner, *Immunol. Ser.* **49**, 155 (1990).
9. R. Halenbeck, E. Kawasaki, J. Wrin, K. Koths, *BioTechnology* **7**, 710 (1989).
10. R. Halenbeck and K. Koths, unpublished observations.
11. J. Jancarik and S.-H. Kim, *J. Appl. Crystallogr.* **24**, 409 (1991).
12. N. Sakabe, *ibid.* **16**, 542 (1983).
13. T. Higashi, *ibid.* **22**, 9 (1989).
14. W. Steigemann, thesis, Technische Universität München (1974).
15. B. C. Wang, *Methods Enzymol.* **115**, 90 (1985).
16. J. M. Cox, *J. Mol. Biol.* **28**, 151 (1967). The relation between the two molecules is described by the spherical angles $\phi = 25.2°$, $\psi = 167.2°$, $\kappa = 180.0°$, and a translation of 141.5, −5.9, and 361.2 Å, respectively, in an orthogonal coordinate system described by *a*, *b*, and *c*. The noncrystallographic symmetry axis was refined with program RHOREF written by P. Chakravarti and D. Rees at UCLA.
17. G. Bricogné, *Acta Crystallogr.* **32**, 832 (1976).
18. An envelope for noncrystallographic symmetry averaging was determined by inspecting the electron density map on the graphics screen and filling up the regions of density believed to correspond to one dimer with dummy atoms.
19. T. A. Jones, *J. Appl. Crystallogr.* **11**, 268 (1978).
20. A. T. Brünger, *XPLOR, A System for Crystallography and NMR, 2.1 Manual* (Yale University, New Haven, CT, 1990).
21. J. Stein, G. V. Borzillo, C. W. Rettenmeier, *Blood* **76**, 1308 (1990).
22. B. Lee and F. M. Richards, *J. Mol. Biol.* **55**, 379 (1971). Solvent accessibility was calculated by using Lee and Richards' algorithm with a probe radius of 1.4 Å.
23. S. R. Presnell and F. E. Cohen, *Proc. Natl. Acad. Sci. U.S.A.* **86**, 6592 (1989).
24. K. Diederichs, T. Boone, P. A. Karplus, *Science* **254**, 1779 (1991).
25. A. M. de Vos, M. Ultsch, A. A. Kossiakoff, *ibid.* **255**, 306 (1992).
26. S. S. Abdel-Meguid *et al.*, *Proc. Natl. Acad. Sci. U.S.A.* **84**, 6434 (1987).
27. R. Powers *et al.*, *Science* **256**, 1673 (1992).
28. J. F. Bazan, *Cell* **65**, 9 (1991).
29. ———, *Proc. Natl. Acad. Sci. U.S.A.* **87**, 6934 (1990).
30. Y. Yarden and A. Ullrich, *Annu. Rev. Biochem.* **57**, 443 (1988).
31. Figures 2, A and C, and 3 were prepared with the program MOLSCRIPT [P. J. Kraulis, *J. Appl. Crystallogr.* **24** (1991)].
32. We thank P. A. Karplus and A. M. deVos for GM-CSF and GH coordinates, respectively. We gratefully acknowledge Chiron Corporation, National Science Foundation (BBS 87-20137), and Department of Energy for a grant, equipment support, and computing support, respectively. The Cα coordinates will be deposited in the Brookhaven Protein Data Bank.

15 June 1992; accepted 20 August 1992

Consequences of Replication Fork Movement Through Transcription Units in Vivo

Sarah French

To examine the basis for the evolutionary selection for codirectionality of replication and transcription in *Escherichia coli*, electron microscopy was used to visualize replication from an inducible ColE1 replication origin inserted into the *Escherichia coli* chromosome upstream (5′) or downstream (3′) of *rrnB*, a ribosomal RNA operon. Active *rrnB* operons were replicated either in the same direction in which they were transcribed or in the opposite direction. In either direction, RNA polymerases were dislodged during replication. When replication and transcription were codirectional, the rate of replication fork movement was similar to that observed in nontranscribed regions. When replication and transcription occurred in opposite directions, replication fork movement was reduced.

RNA polymerases (RNAPs) and DNA polymerases (DNAPs) are highly processive enzyme complexes that use the same DNA template to guide their activities. Unless transcription and replication are spatially or temporally separated, there may be times in the cell cycle when RNAPs and DNAPs must compete for right-of-way along the same stretch of DNA. Replication in *Escherichia coli* is initiated bidirectionally from a single site, *oriC*. In rich medium, the time it takes to replicate the chromosome is longer than the doubling time of the cell (*1*). In order for each daughter cell to receive a full chromosomal complement under these conditions, a new round of replication must be initiated before the previous round is completed. Six or more replication forks may, therefore, be present on the chromosome at the same time. Rapid cell growth also requires high amounts of gene expression to provide adequate amounts of cellular precursors. Because DNA replication in *E. coli* proceeds at 20 times the rate of transcription (*2*, *3*), collisions between RNAPs and DNAPs can occur. How are these conflicts resolved?

The bacterial chromosome apparently is organized to avoid head-on collisions between DNAPs and RNAPs (*4*, *5*). Codirectionality of replication and transcription predominates, especially for genes that are frequently transcribed (*5*). Of the genes known to encode protein synthesis machinery, 90% are transcribed in the same direction in which they are replicated. It has been postulated that, if replication and transcription are codirectional, replication forks can follow slowly behind RNAPs until transcription is terminated (*5*). At that point, replication can continue at its normal speed. Head-on collisions would be more difficult to resolve, consistent with an apparent evolutionary selection against their occurrence.

Researchers' efforts to visualize the interaction between replication and transcription (*6*) have been subject to uncertainties about where the replication originated, what the transcriptional state of the DNA was before replication, and whether observed replication forks were moving or stationary. I have inserted here an inducible replication origin into the *E. coli* chromosome in a region that is well characterized, easily recognized, and frequently transcribed. Using the Miller chromatin spreading technique (*7*, *8*) in conjunction with electron microscopy, I observed the positions of replication forks relative to transcribing RNAPs after induction of replication.

The inducible replication origin was inserted upstream or downstream of *rrnB*. One of seven ribosomal RNA (rRNA) operons in *E. coli*, *rrnB* is a good template over which to view the interaction of replication and transcription because it is long [5.4 kb (*9*)] and actively transcribed [12 RNAPs per kilobase (*7*)]. The rRNA operons are easily recognized in chromatin spreads by their unique morphology (Figs. 1A and 2A). They are densely packed with RNAPs, and the processing of transcripts between the 16*S* and 23*S* cistrons (*10*) gives rise to two gradients of increasing transcript length. The *rrnB* operon can be identified by its proximity to the *tufB* transcription unit 4 kb downstream (*7*). No other *rrn* operon

Department of Biology, University of Virginia, Charlottesville, VA 22903.

has a similar pattern of downstream transcription.

Plasmid pLA512 (*11*) provided the inducible replication origin. A *lac*UV5 promoter replaces the primer promoter of the ColE1 replication origin in pLA512. Replication in pLA512 is unidirectional, primed by read-through transcription from *lac*UV5, and requires induction by isopropylthiogalactoside (IPTG). An advantage of unidirectional replication is that the origin can be used as a reference point from which the extent of replication can be measured. Although ColE1 replication is primed by RNAP and initiated with DNAP I, a switch to the normal *E. coli* replicative DNAP (DNAP III) occurs less than 1 kb from the ColE1 origin (*12*). Replication from pLA512 was therefore considered an adequate model for chromosomal replication.

Using homologous recombination, I inserted the entire pLA512 plasmid into the *E. coli* chromosome (*13*). Upstream of *rrnB*, pLA512 was inserted into *btuB* and oriented so that replication and *rrnB* transcription occurred in the same direction (strain CF78). Downstream from *rrnB*, pLA512 was inserted into *birA* so that inducible replication and *rrnB* transcription proceeded in opposite directions and were oriented toward each other (strain CF95).

Strains CF78 and CF95 were grown to mid-log phase (optical density at 550 nm was 0.3 to 0.5) in LB medium (*14*) at 37°C. IPTG (0.1 mM) was added, and 4 to 6 min later the cultures were prepared for electron microscopy. Replication from pLA512 was not completely synchronous, but sufficient numbers of origins fired within a few minutes of IPTG addition for interactions between replication and transcription to be analyzed. In strain CF78, 25% (n = 78) and 40% (n = 86) of observed pLA512 origins had fired after 4- and 6-min exposures to IPTG, respectively (*15*). In CF95, 24% (n = 25) and 37% (n = 125) of the origins had fired after 4 and 6 min, respectively. The imprecise synchrony of pLA512 replication after induction may be explained by the observation that only 5% of ColE1 primer transcripts initiate DNA synthesis in vivo (*16*).

After induction of codirectional replication in strain CF78, replication forks were observed between the pLA512 origin and *rrnB* (Fig. 1A) or within *rrnB* (Fig. 1B), but in most cases (Table 1), the replication fork had already traversed *rrnB* (Fig. 1C). Whenever a replication fork was observed in *rrnB*, RNAPs were present in front of the replication fork but were absent from the newly replicated strands in the 2 to 3 kb immediately behind the fork (n = 4) (Fig. 1B). Repopulation of *rrnB* with RNAPs could be observed after the replication fork had passed further downstream. Eight *rrnB* daughter pairs (n = 34) were observed that were only partially repopulated by RNAPs (Fig. 1C). All displayed normal transcription complexes at their 5′ ends but lacked transcription complexes at their 3′ ends. Where the position of the moving fork could be estimated (n = 4), the extent of repopulation of *rrnB* paralleled the time elapsed since replication. Transcription patterns on daughter duplexes were symmetric whether or not *rrnB* was fully repopulated with RNAPs.

A comparison of replication fork positions in the *rrnB* region of CF78 4 and 6 min after induction of replication (Table 1) suggests that replication fork movement was not slowed by RNAPs transcribing *rrnB*. In *E. coli*, the rate of replication fork movement is estimated to be 1 kb/s (*2*), whereas the transcription elongation rate for rRNA is 42 nucleotides per second (*3*). If replication forks were constrained to follow behind transcribing RNAPs, it would take 2.2 min rather than 5 to 6 s to

Table 1. Positions of replication forks in strains CF78 and CF95 4 and 6 min after induction of pLA512 replication with IPTG.

Strain	Exposure to IPTG (min)	Numbers of replication forks (%)		
		Between pLA512 origin and *rrnB*	In *rrnB*	Beyond *rrnB*
CF78	4	3 (16%)	2 (11%)	14 (74%)
	6	3 (9%)	2 (6%)	30 (86%)
CF95	6	6 (16%)	26 (68%)	6 (16%)

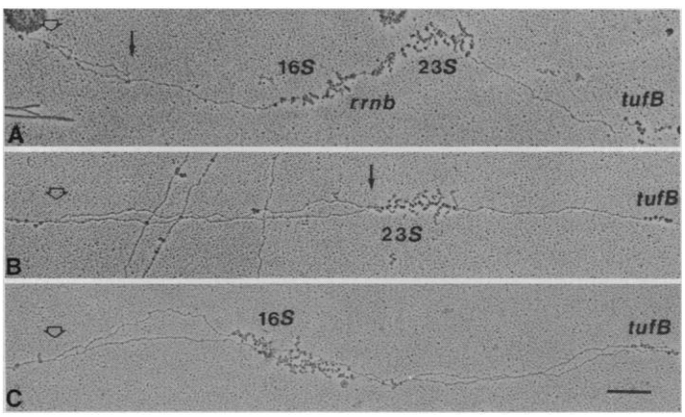

Fig. 1. Electron micrographs of strain CF78 after induction of replication with IPTG. Open arrow, pLA512 origin. Solid arrow, advancing replication fork. Bar represents 1 kb. (**A**) Replication fork approaching *rrnB*. (**B**) Replication fork in *rrnB*. Failure to observe a large protein complex at the replication fork may be due to loss of replication proteins during chromatin spreading and the low electron density of DNAP. (**C**) Reinitiation of transcription at *rrnB*. Replication has proceeded downstream of *rrnB*. Insufficient time has elapsed for transcription of the 23*S* cistron to be completed. The downstream replication fork could not be located because replication had proceeded beyond the *rpoBC* operon, where this grid-square ended.

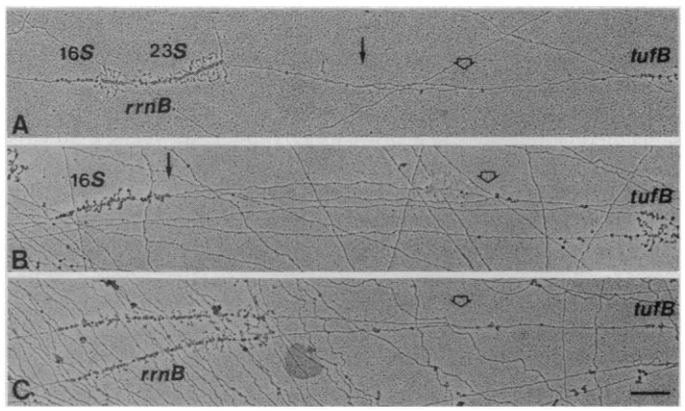

Fig. 2. Electron micrographs of strain CF95 after induction of replication with IPTG. The distance between *tufB* and *rrnB* has increased to 9.3 kb because of the insertion of pLA512 at *birA*. Unidirectional replication from pLA512 proceeds toward *rrnB* and is in the direction opposite to *rrnB* transcription. Open arrow, pLA512 origin. Solid arrow, moving replication fork. Bar represents 1 kb. (**A**) Replication fork approaching *rrnB*. (**B**) Replication fork in *rrnB*. (**C**) The *rrnB* operon can be completely replicated in the direction opposite to that in which it is transcribed. Because transcription is disrupted during replication, the transcriptional activity observed here must have been initiated after passage of the replication fork.

replicate *rrnB*. From sequence analysis, the distance from the pLA512 origin to *rrnB* in CF78 is 4.2 kb (*17*, *18*) (4.8 ± 0.5 kb; mean ± SD; $n = 44$; by electron microscopy) and is similar to the length of *rrnB* [5.4 kb (9)]. The number of replication forks observed in *rrnB* was similar to that observed between *rrnB* and the origin, suggesting that the rate of replication fork movement was similar in both nontranscribed and transcribed regions. Replication forks did not accumulate in *rrnB*, and most replication that was observed had proceeded downstream.

The exact positions of forks that had replicated *rrnB* could generally not be determined because daughter strands became obscured by cell debris or the edge of a sample grid was reached (5 to 60 kb downstream) before the replication fork was encountered. Strands downstream of 22 *rrnB* pairs were photographed; 7 could be followed for more than 40 kb, 13 for more than 25 kb.

The absence of RNAPs behind replication forks that move through *rrnB* faster than RNAPs transcribe the operon, combined with the normal appearance of transcription complexes in front of the forks, suggests that RNAPs are dislodged from the DNA during replication. Repopulation of *rrnB*, as well as of the less highly transcribed *tufB* and *rpoBC* operons (*7*), by RNAPs occurred in a promoter-proximal to promoter-distal fashion, consistent with the idea of reinitiation of transcription occurring at an operon that is cleared of transcription complexes.

Dissociation of stationary RNAPs from a DNA template during replication has been observed in vitro with bacteriophage T4 replication proteins (*19*) and required the presence of a T4-encoded helicase (dda). Similar to *E. coli*, replication rates in the in vitro T4 system were much greater than transcription rates, and replication and transcription were codirectional. In the absence of dda helicase, replication forks were blocked by promoter-bound RNAPs, but they could follow slowly behind transcribing RNAPs. In the presence of dda helicase, replication rates were rapid, and rates were similar with or without RNAPs or transcription. It is possible that, as in the case of T4, a helicase is involved in the efficient replication of active transcription units in *E. coli*.

Between the 14th and 15th mitotic cycle, in *Drosophila melanogater* embryos (cellular blastoderm), *Ubx* transcription complexes apparently are not disrupted during chromosome replication (*20*). Because the rate of replication is similar to the rate of transcription in these cells (*20*, *21*), replication forks may passively follow RNAPs without difficulty.

In strain CF95, replication from pLA512 is initiated between *tufB* and *rrnB* (Fig. 2A), and the active replication fork moves toward the 3′ end of *rrnB*. In contrast to observations in yeast, which suggest that 3′ ends of rRNA genes are effective barriers to replication forks approaching from downstream (*22*), replication forks originating from pLA512 entered the 3′ end of *rrnB* (Fig. 2B) and were able to completely replicate the operon (Fig. 2C). Transcription complexes of normal density and appearance were observed in front of replication forks extending from 0.1 to 5.1 kb ($n = 26$) into *rrnB* but were absent from the replicated portion of *rrnB* behind the forks. In five replication bubbles, one to three particles, but no fibrils suggestive of transcripts, were associated with *rrnB*. It appears that, regardless of the relative directions of replication and transcription, RNAPs are dislodged during replication.

In CF95, the distance from the pLA512 origin to *rrnB* is 4.7 kb by sequence analysis (*17*, *23*), 5.2 ± 0.5 kb (mean ± SD; $n = 32$) by electron microscopy, and similar to that in CF78. The proportion of replication forks observed between pLA512 and *rrnB* in CF78 and CF95 was similar (Table 1), indicating that rates of replication outside active transcription units were the same in these two strains and were independent of the direction of replication. The relative direction of replication and transcription, however, drastically affected the rate at which *rrnB* was replicated. In CF95, 6 min after IPTG addition most replication from pLA512 had not yet progressed beyond *rrnB* (Table 1).

Orientation-dependent differences that might contribute to the disparity observed between replication rates for *rrnB* in CF78 and CF95 include changes in protein-protein interactions and altered amounts of supercoiling. When replication and transcription are codirectional, RNAPs and the leading strand DNAP use the coding DNA strand as template, and negative supercoils behind transcribing RNAPs may cancel positive supercoils generated in front of the replication fork (*24*). When replication and transcription occur in opposite directions, the leading strand DNAP replicates the noncoding strand, and direct head-on collisions occur between RNAPs and the *dnaB* helicase traveling on the coding strand. RNAPs and replication forks now generate positive supercoils toward one another. If a large increase in positive supercoil density between converging polymerase complexes is responsible for retarding replication fork movement in CF95, this effect occurs only over short distances. Replication forks did not accumulate between pLA512 and *rrnB*, and most replication forks observed in *rrnB* were within 200 bp or less of the nearest RNAP. The close approach of replication forks to RNAPs agrees with observations that the propagation of transcriptionally induced supercoils in vivo is limited (*25*).

The location of pLA512 in CF95 allowed the study of the interaction of replication and transcription only at *rrnB*; therefore, conclusions cannot be directly drawn about the effect that moderately active or short transcription units would have on replication forks approaching from downstream. Placement of pLA512 downstream of *rpoBC* so that interactions can be observed through *rpoBC* and *tufB*, as well as through *rrnB* should clarify this matter. Although transcription is disrupted during replication, the degree of disruption is dependent on the relative orientation of replication and transcription. Thus, the orientation of a gene may ultimately affect its expression.

REFERENCES AND NOTES

1. C. E. Helmstetter and S. Cooper, *J. Mol. Biol.* **31**, 507 (1968); S. Cooper and C. E. Helmstetter, *ibid.*, p. 519; K. Skarstad, H. B. Steen, E. Boye, *J. Bacteriol.* **163**, 661 (1985); R. Allman, T. Schjerven, E. Boye, *ibid.* **173**, 7970 (1991).
2. Rates are from S. Hirose, S. Hiraga, and T. Okazaki [*Mol. Gen. Genet.* **189**, 422 (1983)] and calculated from replication times (*1*) and chromosome length and from timing of hemimethylation [J. L. Campbell and N. Kleckner, *Cell* **62**, 967 (1990)].
3. S. L. Gotta, O. L. Miller, Jr., S. L. French, *J. Bacteriol.* **173**, 6647 (1991); D. J. Jin, R. R. Burgess, J. P. Richardson, C. A. Gross, *Proc. Natl. Acad. Sci. U.S.A.* **89**, 1453 (1992).
4. M. Nomura, E. A. Morgan, S. R. Jaskunas, *Annu. Rev. Genet.* **11**, 297 (1977).
5. B. J. Brewer, *Cell* **53**, 679 (1988); in *The Bacterial Chromosome*, K. Drlica and M. Riley, Eds. (American Society for Microbiology, Washington, DC, 1990), pp. 61–83.
6. S. L. McKnight, thesis, University of Virginia (1978); L. D. Saffer and O. L. Miller, Jr., *Mol. Cell. Biol.* **6**, 1148 (1986); Y. N. Osheim, O. L. Miller, Jr., A. L. Beyer, *ibid.* **8**, 2811 (1988).
7. S. French and O. L. Miller, Jr., *J. Bacteriol.* **171**, 4207 (1989).
8. Cells were prepared for electron microscopy with the Miller chromatin spreading technique as described (*7*), with one modification: dispersed cell contents were centrifuged onto carbon-coated, copper electron microscope grids through a cushion of 0.1 M sucrose and 1% formalin. Sample preparation effectively inhibits transcription elongation [S. Gotta, thesis, University of Virginia (1991)] and, by inference, replication, which is more cold-sensitive.
9. J. Brosius *et al.*, *J. Mol. Biol.* **148**, 107 (1981).
10. S. Hofmann and O. L. Miller, Jr., *J. Bacteriol.* **132**, 718 (1977).
11. N. Panayotatos, *Nucleic Acids Res.* **12**, 2641 (1984).
12. K. Backman *et al.*, *Cold Spring Harbor Symp. Quant. Biol.* **43**, 69 (1978).
13. I used the Aat II site of pLA512 for cloning either a 0.8-kb internal Sal I fragment of *btuB* from pAG1 [M. D. Lundrigan, W. Köster, R. J. Kadner, *Proc. Natl. Acad. Sci. U.S.A.* **88**, 1479 (1991)] or a 2.25-kb Bam HI–Bgl II fragment from pAB11 containing the intact *birA* gene [D. F. Barker and A. M. Campbell, *J. Mol. Biol.* **146**, 469 (1981)]. Transformants of W3110 *lacI*^{q} (L8), Δ*trp*(EDCBA)2 were selected for by the acquisition of carbenicillin resistance in the absence of IPTG. I verified the insertion of pLA512 into *btuB* by screening transformants for resistance to phage

BF23, which used *btuB* as a cell surface receptor to gain entry into *E. coli*. Because *birA* is an essential gene, recombinants at *birA* were screened by electron microscopy.
14. T. Maniatis, E. F. Fritsch, J. Sambrook, *Molecular Cloning: A Laboratory Manual* (Cold Spring Harbor Laboratory, Cold Spring Harbor, NY, 1982), p. 68.
15. Sample size (*n*) for measurements of different features in a given replication time period varied because debris or tangled strands often prevented measurement of all features on every micrograph.
16. N. Inoue and H. Uchida, *J. Bacteriol.* **173**, 1208 (1991).
17. J. Devereux, P. Haeberli, O. Smithies, *Nucleic Acids Res.* **12**, 387 (1984).
18. K. Heller and R. J. Kadner, *J. Bacteriol.* **161**, 904 (1985).
19. P. Bedinger, M. Hochstrasser, C. V. Jongeneel, B. M. Alberts, *Cell* **34**, 115 (1983).
20. A. W. Shermoen and P. H. O'Farrell, *ibid.* **67**, 303 (1991).
21. A. B. Blumenthal, H. J. Kiegstein, D. S. Hogness, *Cold Spring Harbor Symp. Quant. Biol.* **38**, 205 (1973).
22. B. J. Brewer and W. L. Fangman, *Cell* **55**, 637 (1988); M. H. K. Linskens and J. A. Huberman, *Mol. Cell. Biol.* **8**, 4927 (1988).
23. P. K. Howard, J. Shaw, A. J. Otsuka, *Gene* **35**, 321 (1985).
24. L. F. Liu and J. C. Wang, *Proc. Natl. Acad. Sci. U.S.A.* **84**, 7024 (1987).
25. R. Rahmouni and R. D. Wells, *J. Mol. Biol.* **223**, 131 (1992).
26. I thank N. Panayotatos for plasmid pLA512, R. Kadner for pAG1, A. Campbell for pAB11, M. Sikes for carbon-coated microscope grids, and O. L. Miller, Jr., for the opportunity to work in his laboratory where these experiments were conducted. I also thank A. Beyer, R. Kadner, and Y. Osheim for helpful comments on the manuscript. Supported by PHS grant GM 21020 from the NIH.

15 June 1992; accepted 1 September 1992

Induction of Mucosal and Systemic Immunity to a Recombinant Simian Immunodeficiency Viral Protein

T. Lehner,* L. A. Bergmeier, C. Panagiotidi, L. Tao, R. Brookes, L. S. Klavinskis, P. Walker, J. Walker, R. G. Ward, L. Hussain, A. J. H. Gearing, S. E. Adams

Heterosexual transmission through the cervico-vaginal mucosa is the principal route of human immunodeficiency virus (HIV) infection in Africa and is increasing in the United States and Europe. Vaginal immunization with simian immunodeficiency virus (SIV) had not yet been studied in nonhuman primates. Immune responses in macaques were investigated by stimulation of the genital and gut-associated lymphoid tissue with a recombinant, particulate SIV antigen. Vaginal, followed by oral, administration of the vaccine elicited three types of immunity: (i) gag protein p27–specific, secretory immunoglobulin A (IgA) and immunoglobulin G (IgG) in the vaginal fluid, (ii) specific $CD4^+$ T cell proliferation and helper function in B cell p27-specific IgA synthesis in the genital lymph nodes, and (iii) specific serum IgA and IgG, with $CD4^+$ T cell proliferative and helper functions in the circulating blood.

Vaginal transmission of SIV has been achieved experimentally in macaques, resulting in the development of an acquired immunodeficiency syndrome (AIDS)–like syndrome (*1*). This route of infection resembles heterosexual transmission of HIV in humans. Although systemic immunization strategies have protected against intravenous challenges with infectious SIV (*2*), they have not prevented vaginal transmission (*1*). In view of these observations and the prevalence of heterosexual transmission of HIV in humans, the development of a simian model of vaccination that can prevent genital transmission of SIV has been emphasized (*3*).

We have shown that protein p1, encoded by the yeast retrotransposon Ty, can be used as a carrier for recombinant antigens and that p1 fusion proteins self-assemble into hybrid virus-like particles (Ty-VLP) (*4*). Systemic immunization studies demonstrated that hybrid particles that carry the SIV gag protein p27 (SIV p27:Ty-VLP) induce both circulating antibody and T cell responses in macaques (*4*). Administration of $SIVmac_{251}$ whole, inactivated vaccine or synthetic peptides by the mucosal route did not induce an effective immune response (*5*). We therefore attempted to use SIV p27:Ty-VLP to stimulate the mucosal-associated lymphoid tissue (*6*). The SIV p27:Ty-VLP was conjugated to the GM1 ganglioside receptor–binding subunit of cholera toxin (CTB), which has potent mucosal adjuvant properties (*7*). We used two separate immunization regimes to assess the p27:Ty-VLP/CTB vaccine that was administered by nontraumatic vaginal and oral instillation. Three macaques received two oral, followed by three vaginal, administrations (O-V), and four macaques received two vaginal, followed by three oral, administrations (V-O) of the vaccine. Four macaques were used as controls by administration of p27:Ty-VLP without CTB, p27 conjugated to CTB (p27/CTB), or p27 alone, all by the O-V route to one macaque each, or by administration of Ty-VLPs conjugated to CTB (Ty-VLP/CTB) by the V-O route to one macaque.

Sequential examination of vaginal, rectal, salivary, and serum antibodies before and after each of the oral and vaginal immunizations with p27:Ty-VLP/CTB showed that IgA (Fig. 1 and Table 1) and IgG (Fig. 2 and Table 1) were specifically raised to p27 (anti-p27). IgA and IgG anti-p27 in vaginal fluid were found after the first or second oral or vaginal immunization in one macaque in each group. In the other macaques immunized by the O-V route, antibodies increased after the fifth mucosal immunization. The macaques in the second group immunized by the V-O route showed an increase in antibodies after the fourth or fifth mucosal immunization. Similar results were found with serum IgA and IgG, except that these were detected earlier (Figs. 1 and 2). Salivary IgA, but not IgG, appeared early, after the first or second vaginal immunization in the V-O group and to a lesser extent in the O-V group (Table 1). Rectal washings showed anti-p27 IgA in only three out of seven macaques and IgG in one out of seven macaques after the fifth mucosal immunization. Of the four control macaques, those immunized with p27:Ty-VLP, p27 alone, or Ty-VLP/CTB did not show IgA or IgG in vaginal and rectal fluids, whereas p27/CTB elicited some antibodies in vaginal fluid (Figs. 1 and 2). However, all but Ty-VLP elicited serum IgA and IgG anti-p27. Immunization with p27/CTB or p27 also induced salivary IgA and IgG (Table 1). One-way analysis of variance (ANOVA) of vaginal anti-p27 IgA in macaques immunized with p27:Ty-VLP/CTB by the V-O route, as compared with the control group, showed a significant difference ($P = 0.017$), and anti-p27 IgG was also significant ($P = 0.022$). Although vaginal IgA elicited by the O-V sequence of immunization was significant ($P = 0.025$), IgG ($P = 0.44$) did not reach the 5% level of significance. By either sequence of immunization, serum anti-p27 IgA was not significant if the immunized group was compared with the control group ($P = 0.057$ and 0.143) because among the control macaques all but Ty-VLP/CTB elicited serum IgA (Figs. 1 and 2). However, serum

T. Lehner, L. A. Bergmeier, C. Panagiotidi, L. Tao, R. Brookes, L. S. Klavinskis, P. Walker, J. Walker, R. G. Ward, L. Hussain, Division of Immunology, United Medical and Dental School of Guy's and St. Thomas' Hospital, London Bridge, London SE1 9RT, United Kingdom.
A. J. H. Gearing and S. E. Adams, British Bio-technology, Ltd., Brook House, Watlington Road, Cowley, Oxford OX4 5LY, United Kingdom.
*To whom correspondence should be addressed.